Electronic Supplementary Material (ESI) for Materials Advances.

SUPPORT INFORMATION

High-Field/High-Frequency EPR spectroscopy on synthetic melanin: on the origin of carbon-centered radicals

J.V. Paulin[a], A. Batagin-Neto[a,b], B. Naydenov[c], K. Lips[c,d,e], C.F.O. Graeff[a,f,*]

[a] São Paulo State University (UNESP), School of Sciences, Postgraduate Program in Science and Technology of Materials (POSMAT), Bauru, Brazil.

[b] São Paulo State University (UNESP), Campus of Itapeva, Itapeva, Brazil.

[c] Helmholtz-Zentrum Berlin für Materialien und Energie GmbH, Berlin, Germany.

[d] Freie Universität Berlin, Department Physics, Berlin, Germany.

[e] University of Utah, Department of Physics and Astronomy, Salt Lake City, USA.

[f] São Paulo State University (UNESP), School of Sciences, Department of Physics, Bauru, Brazil.

Corresponding author:
carlos.graeff@unesp.br (C.F.O. Graeff)

Table of Contents

SI-1. Possible melanin and sulfonated melanin radical species.

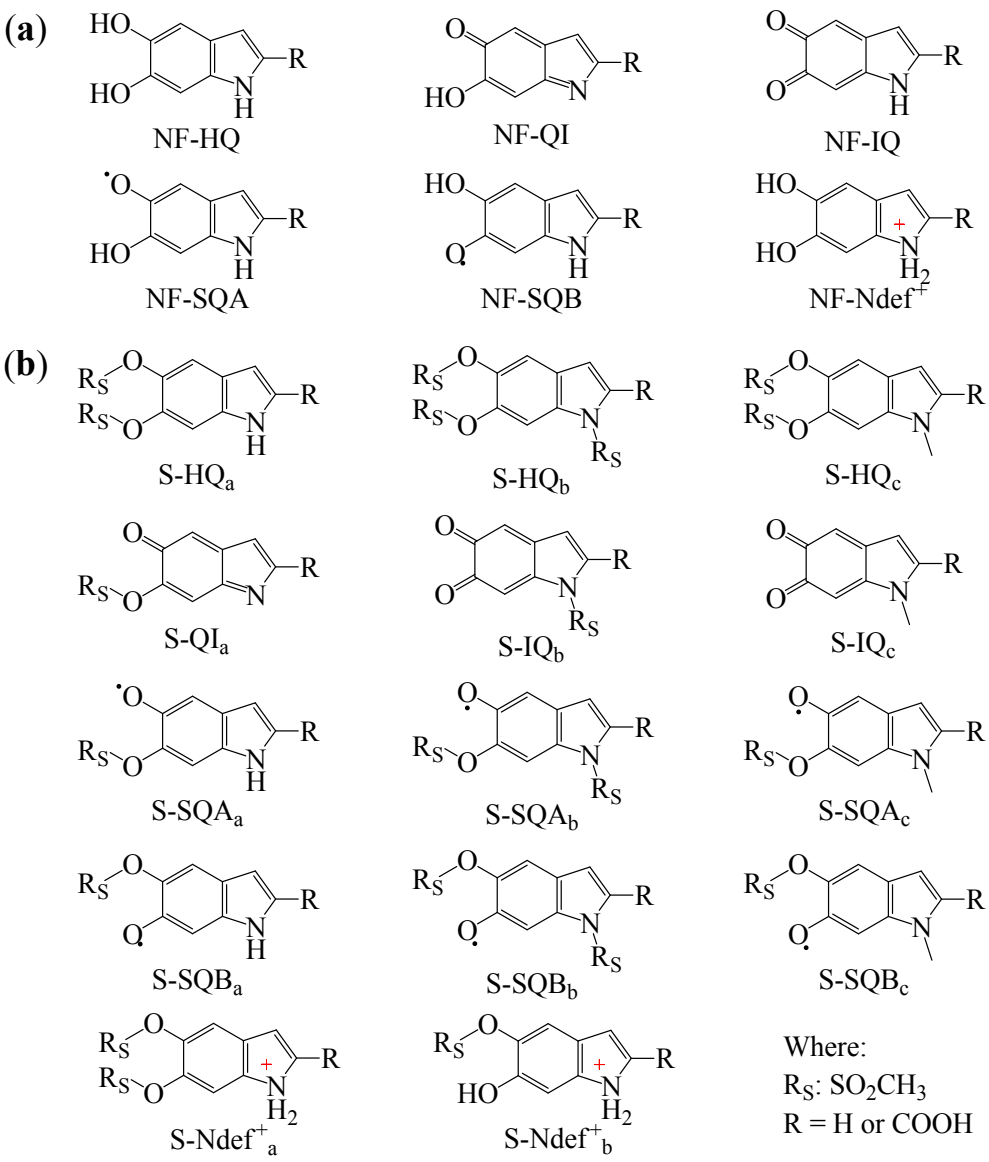

Figure S1. The different units of (a) NF-melanin and (b) S-Melanin.

SI-2. Additional HFEPR analysis

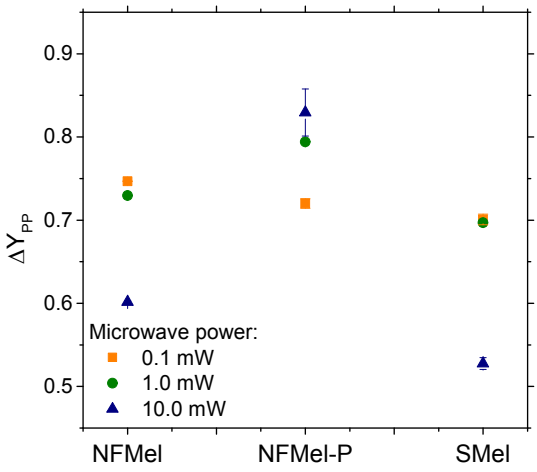

Figure S2. HFEPR signal symmetry (ΔY_{PP}) of NFMel, NFMel-P, SMel. ΔY_{PP} is obtained from the ratio between positive and negative intensities and the closer it is to 1, the more symmetrical the signal is.

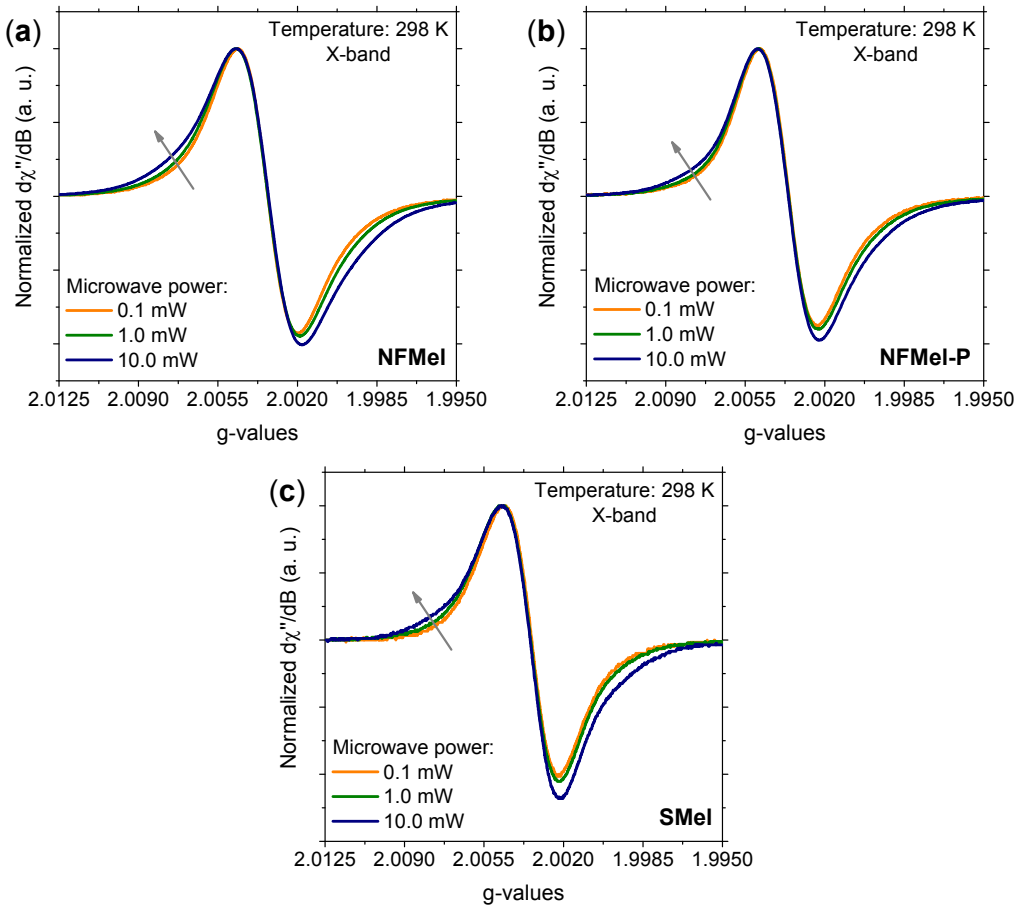

Figure S3. X-band EPR absorption signal of (a) NFMel, (b) NFMel-P and (c) SMel at different microwave powers. The gray arrow indicates the shoulder-like feature increases. Measurements performed in solid-state using an X-band spectrometer MiniScope MS300 (Magnettech) coupled with an Agilent Frequency Counter 53181A RF. For *g* calibration, it was used 2,2-diphenyl-1-picrylhydrazyl (DPPH, g = 2.0036).

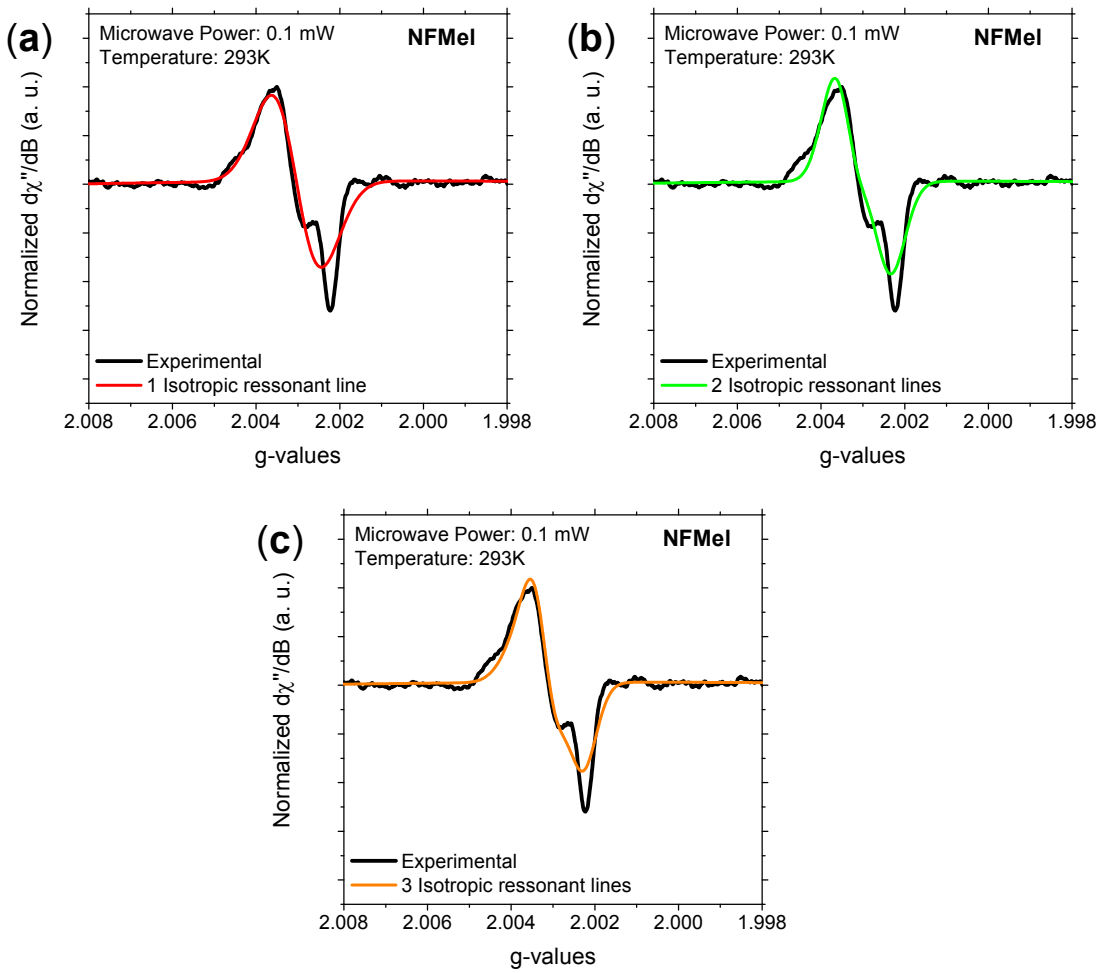

Figure S4. HFEPR absorption signal simulation of NFMel with different isotropic resonant lines at low microwave power (0.1 mW).

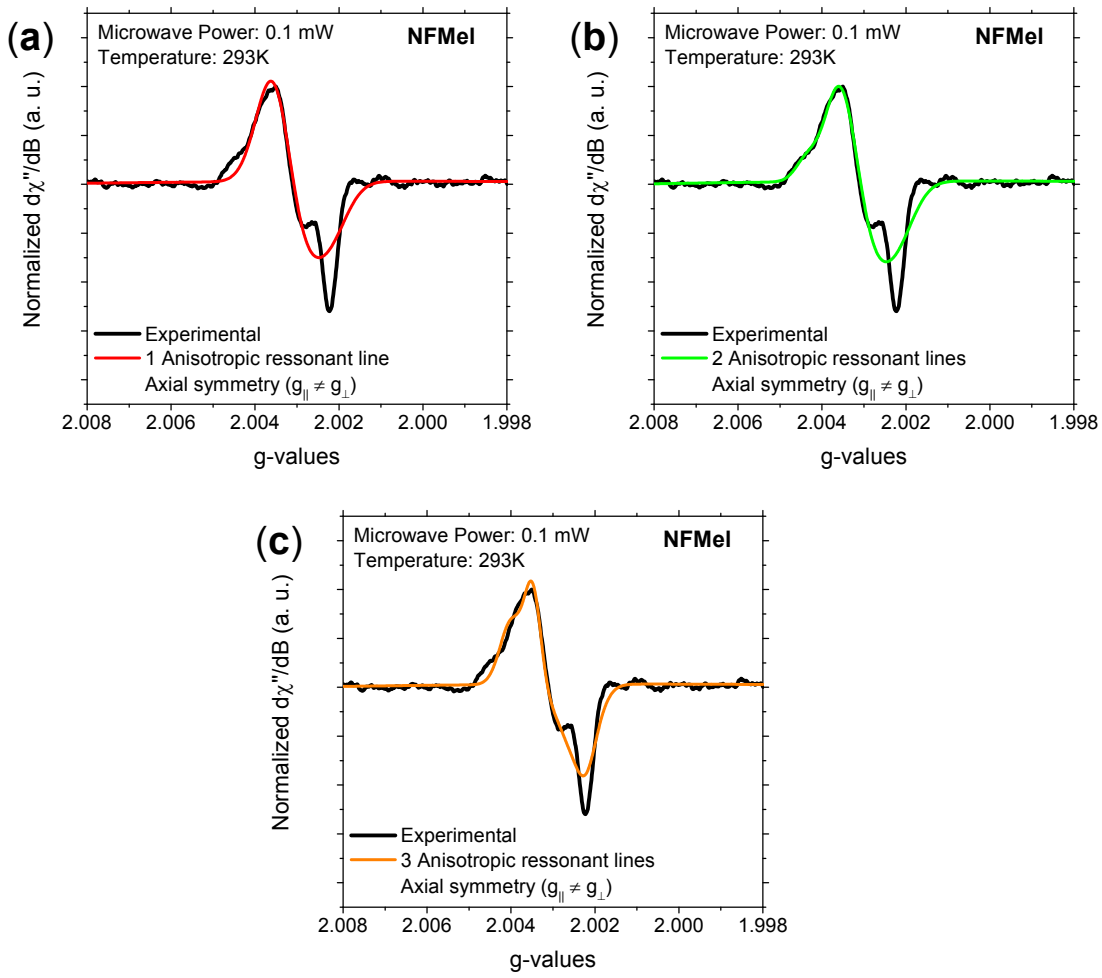

Figure S5. HFEPR absorption signal simulation of NFMel with different anisotropic resonant lines and axial symmetry at low microwave power (0.1 mW).

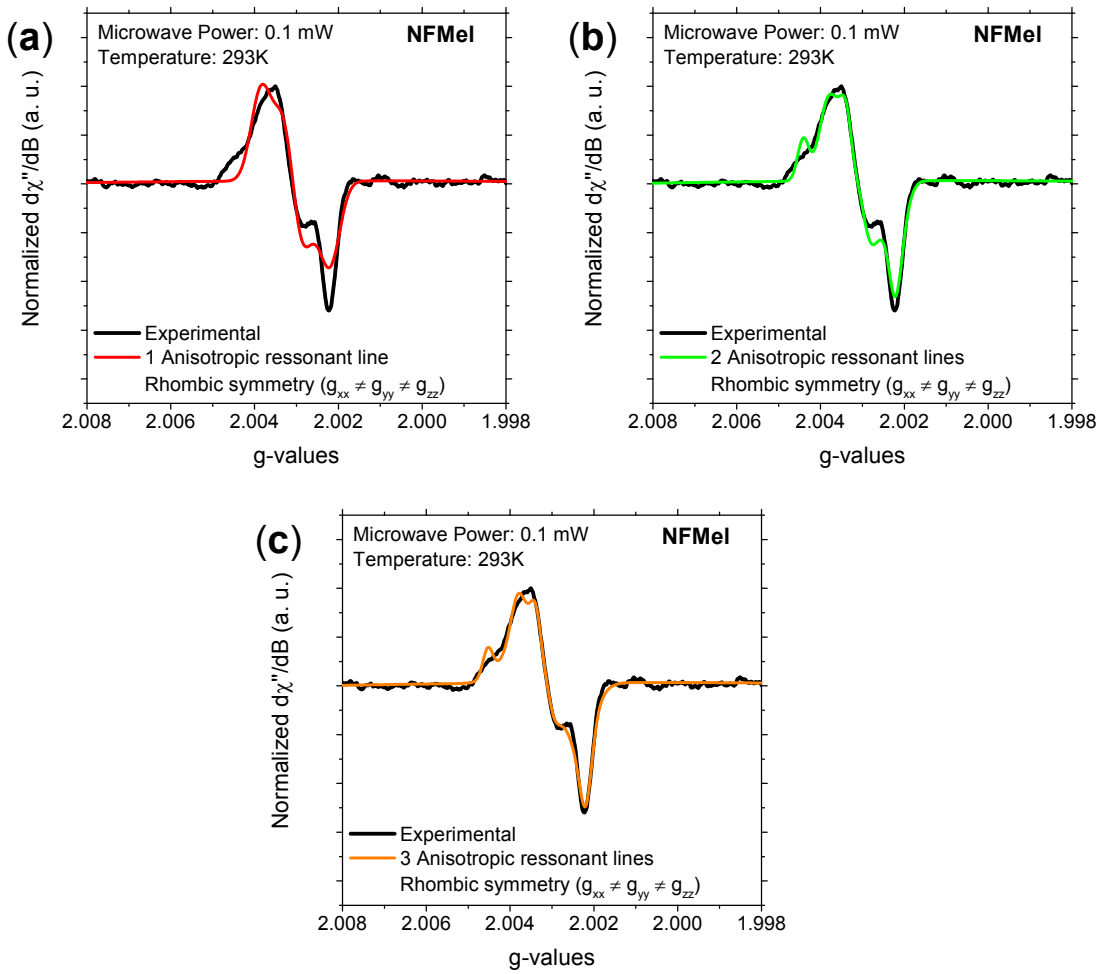

Figure S6. HFEPR absorption signal simulation of NFMel with different anisotropic resonant lines and rhombic symmetry (without *g* strain) at low microwave power (0.1 mW).

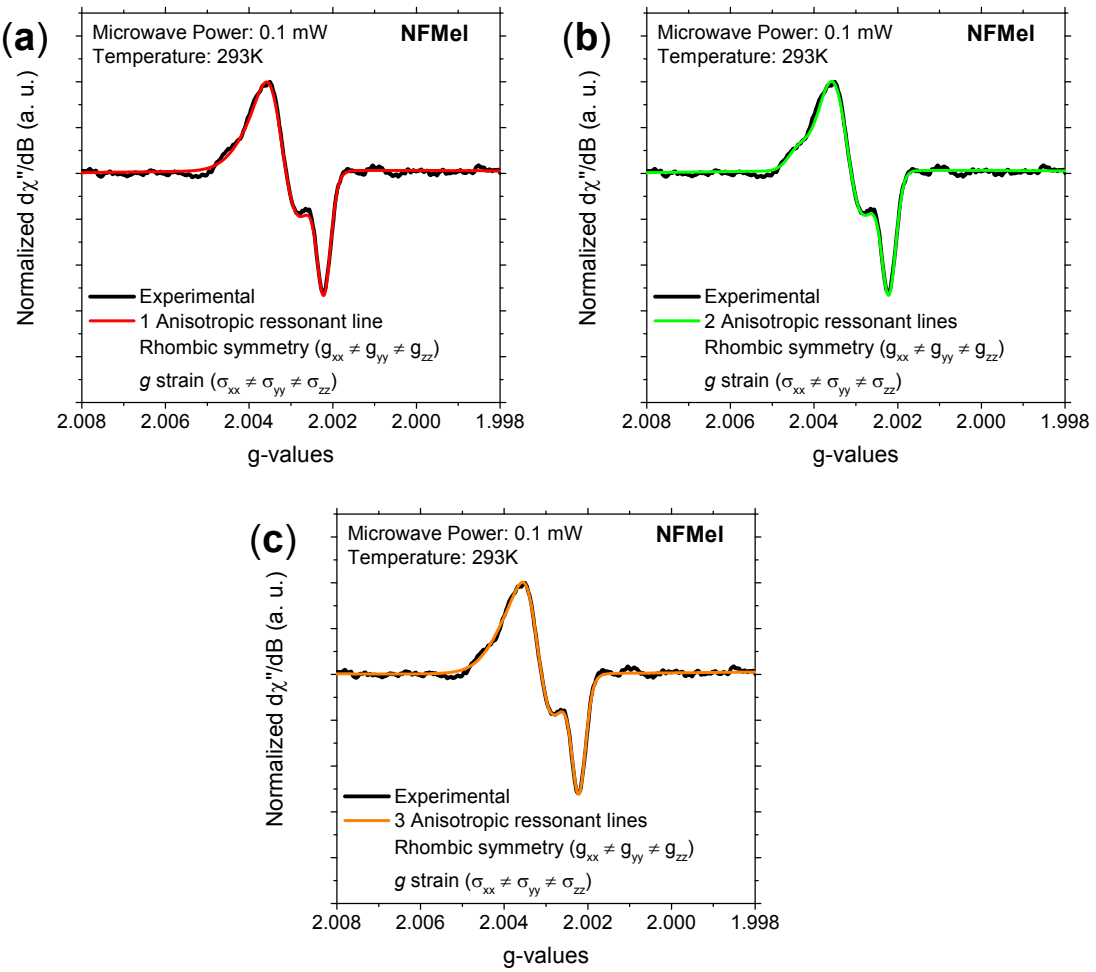

Figure S7. HFEPR absorption signal simulation of NFMel with different anisotropic resonant lines, rhombic symmetry and *g* strain at low microwave power (0.1 mW).

Table S1. Experimentally Determined g-Values for NFMel with Different Resonant Lines.

Resonant Line	g_{xx}	g_{yy}	g_{zz}	g_{iso}
A-I	2.0038	2.0033	2.0023	2.0031
B-I	2.0043	2.0030	2.0023	2.0032
B-II	2.0037	2.0032	2.0022	2.0030
C-I	2.0050	2.0031	2.0023	2.0035
C-II	2.0038	2.0033	2.0023	2.0031
C-III	2.0038	2.0033	2.0022	2.0030

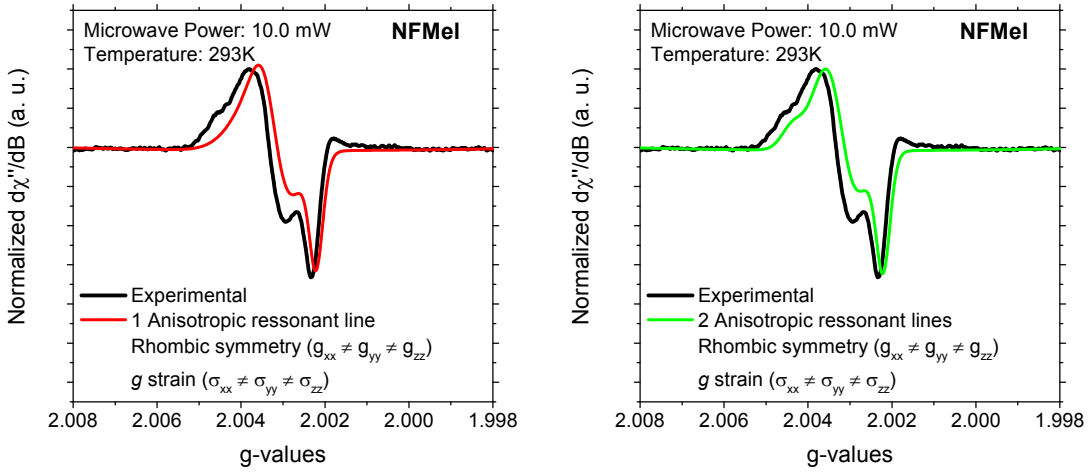

Figure S8. HFEPR absorption signal simulation of NFMel with different anisotropic resonant lines, rhombic symmetry and *g* strain at high microwave power (10.0 mW).

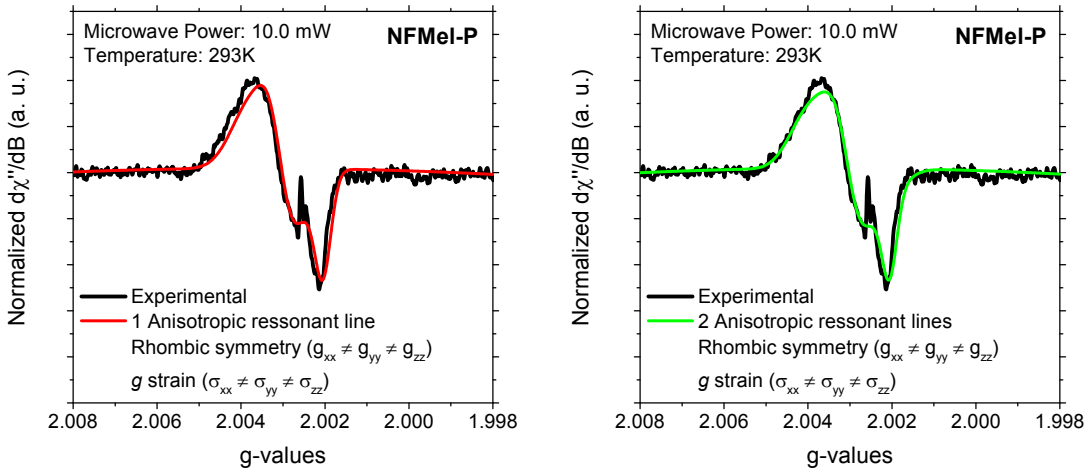

Figure S9. HFEPR absorption signal simulation of NFMel-P with different anisotropic resonant lines, rhombic symmetry and *g* strain at high microwave power (10.0 mW).

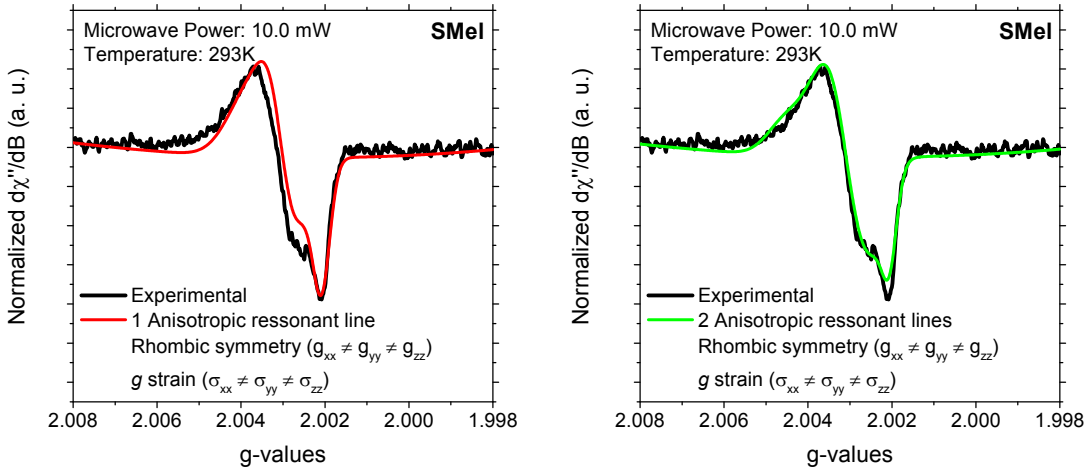

Figure S10. HFEPR absorption signal simulation of SMel with different anisotropic resonant lines, rhombic symmetry and *g* strain at high microwave power (10.0 mW).

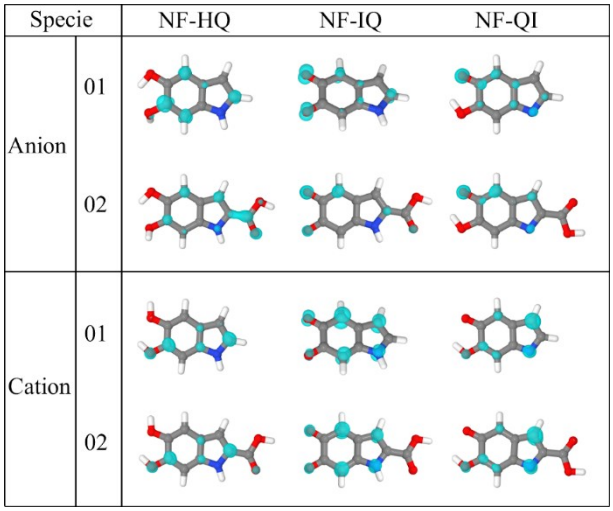

Figure S11. Spin density estimated for charged NF-Melanins.

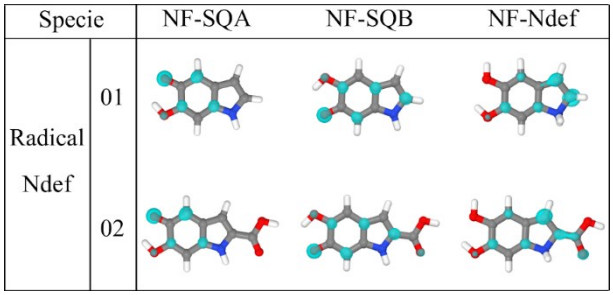

Figure S12. Spin density estimated for SQ radicals and Ndef structures of NF-Melanins.

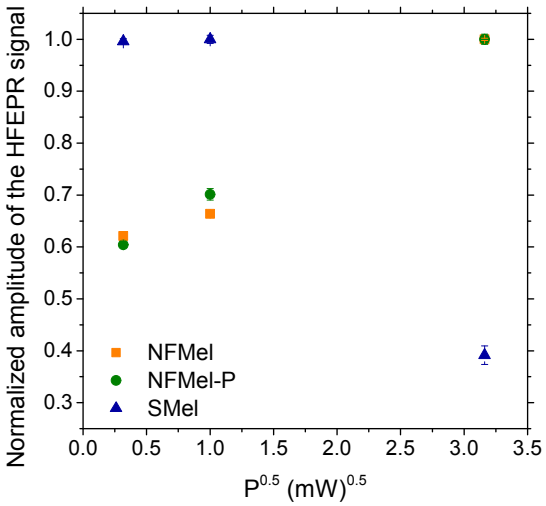

Figure S13. Normalized amplitude as a function of the square root of the power intensity for NFMel, NFMel-P and SMel.

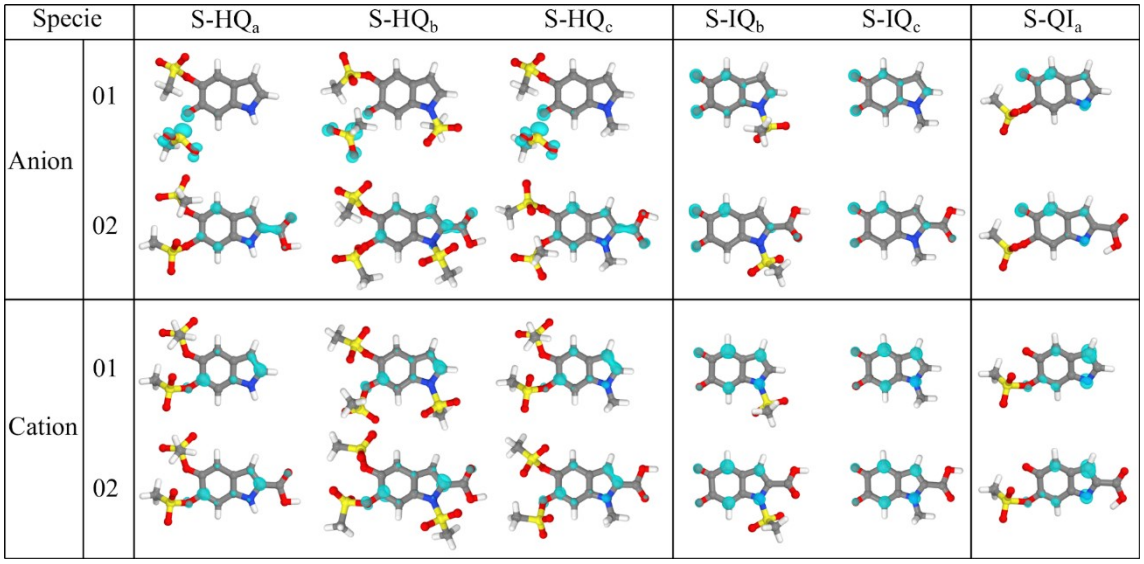

Figure S14. Spin density estimated for charged S-Melanins.

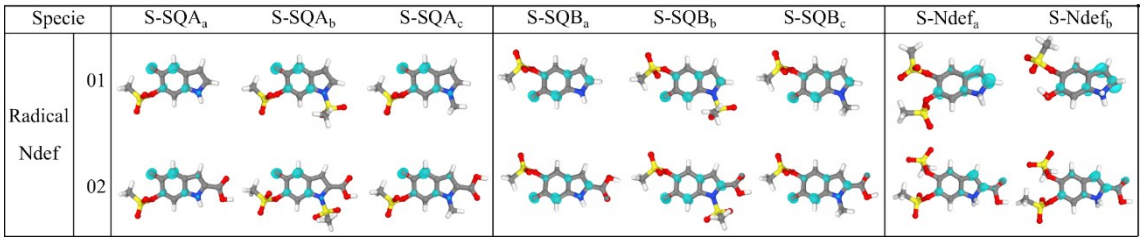

Figure S15. Spin density estimated for SQ radicals and Ndef structures of S-Melanins.

Table S2. Examples of Fitting Parameters of Melanin and Melanin Derivatives.

Melanin sample	Frequency	Symmetry		g Values			Ref.
				Species I	Species II	Species III	
Synthetic melanin (pH 12)	35 GHz	Anisotropic	Axial	2.0054/2.0025	2.0054/2.0030	#	RS1
Synthetic melanin (pH 11)				2.0054/2.0024	2.0054/2.0030	#	
Synthetic melanin (pH 9)				2.0054/2.0025	2.0044/2.0028	#	
Synthetic melanin (pH 6)				2.0052/2.0027	2.0043/2.0029	#	
Synthetic melanin (pH 5)				2.0039/2.0025	2.0041/2.0029	#	
Synthetic melanin (pH 3)				2.0039/2.0025	2.0042/2.0029	#	
DHI-Melanin DHICA-Melanin Synthetic melanin Oxidized synthetic melanin Synthetic melanin (pH acidic) Synthetic melanin (pH neutral) Synthetic melanin (pH alkaline)	9.4 GHz	Isotropic	cylindrical	2.0049	2.0038	2.0026	RS2
Sulfonated melanin Oxidized sulfonated melanin	9.7 GHz	Isotropic	cylindrical	2.0052	2.0043	2.0028	RS3
Synthetic melanin Oxidized synthetic melanin				2.0053	2.0043	2.0027	

Table S3. EPR signal linewidth as a function of frequency.

	ΔH_{PP} (mT)				Ref.
Frequency (GHz)	9.40	35.00	94.04	263.00	
Melanin samples					
Natural melanin (Bovine eye & amphiuma liver)	#	1.78 ± 0.09	#	#	RS4
Hair melanin	#	#	4.48	#	RS5
Dopa-melanin (pH 3)	#	0.82	#	#	RS1
Dopa-melanin (pH 12)	#	0.57	#	#	RS1
Synthetic melanin (Dopa, dopamine, nerepinebeohrine, serotoninm & tryptamine)	#	1.80 ± 0.19	#	#	RS4
5-S-cysteinyldopa melanin	#	#	6.45	#	RS6
NFMel-S	0.45	#	#	6.33	This work
NFMel-6P	0.43	#	#	7.16	This work
Sulfonated melanin	0.41	#	#	6.88	This work

SI-3. Procedure for baseline and phase correction.

Initially, to facilitate the understanding of the process, we create a hypothetical absorption spectrum from $A = exp\left[-\frac{(1-x)^2}{0.005^2}\right]$, Figure SI-1a, as example. The Hilbert transform of the absorption *A* spectrum was used to obtain the dispersion signal *D*. We usually measure the absorption's first derivative. Hence, Figure SI-1b presents the first derivative of the absorption (A') and the first derivative of the dispersion (B').

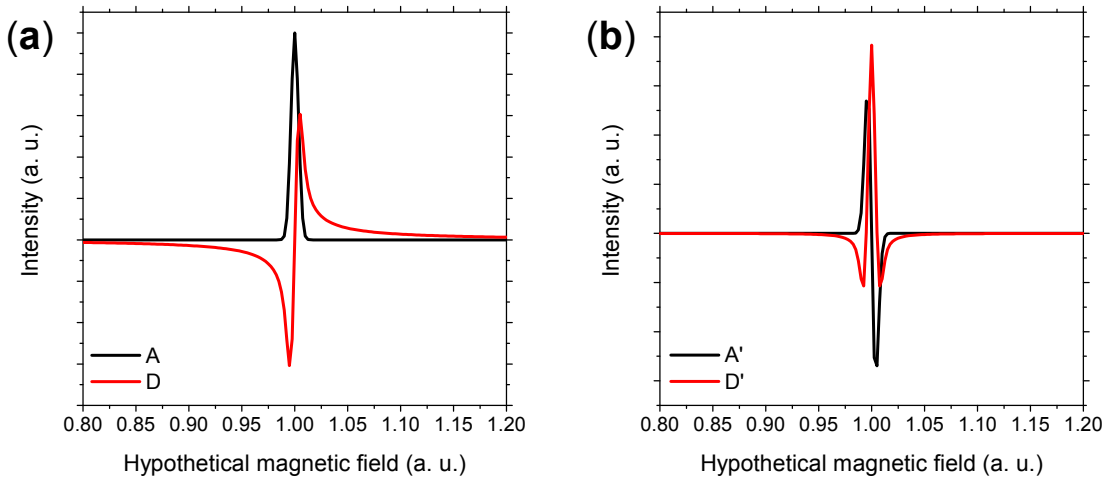

Figure SI-1. (a) Hypothetical absorption *A* and dispersion *D* spectra. (b) The first derivative of the signs in (a).

Figure SI-1 shows the *pure* spectra. However, in our experimental case, there is the possibility that the spectra are a mixture of both absorption and dispersion. Therefore, we create a hypothetical experimental spectrum *S* by taking a linear of A' and D' (I). Additionally, the Hilbert transform of *S* (named H) is given by (II).

$$S = A' + \alpha\, D' \qquad \text{(I)}$$

$$H = D' + \alpha\, A' \qquad \text{(II)}$$

Figure SI-2 shows the resulted spectra for S and H considering α = 0.5.

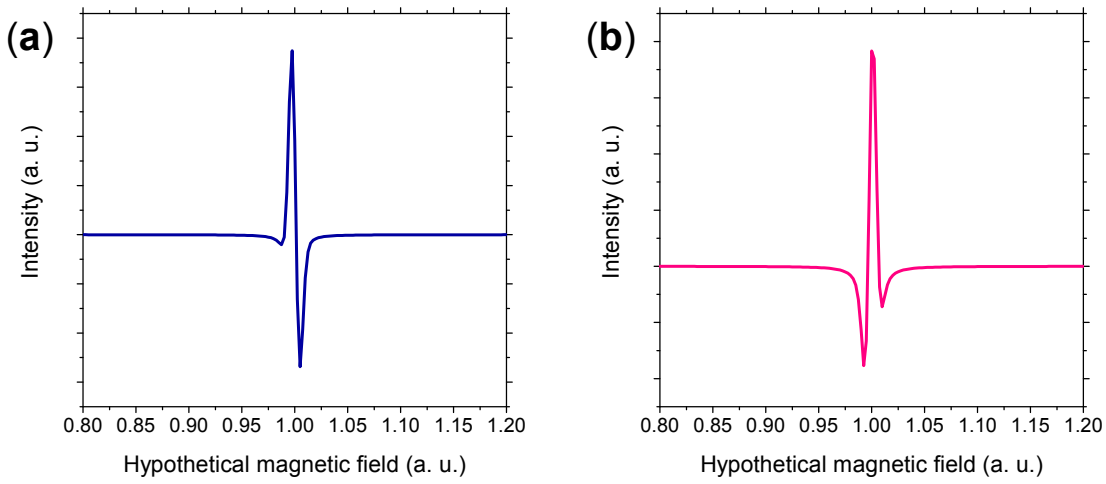

Figure SI-2. (a) Hypothetical experimental spectra S, with α = 0.5, and its (b) Hilbert transform H.

As we intend to do a phase correction to obtain a pure absorption (or its first derivative) of the *experimental* spectra, we need to discover α. Following the methodology reference from Earle *et al.* (RS7), we need to take a linear combination of the S and H. In this case, we got:

$$\begin{gathered} C = S + \beta\, H \\ \Downarrow \\ C = (1 - \alpha\, \beta)\, A' + (\alpha + \beta) D' \end{gathered} \qquad \text{(III)}$$

If,

$$\alpha\, \beta = 1 \Leftrightarrow \beta = \frac{1}{\alpha} \qquad \text{(IV)}$$

then, C is proportional to only D'. This means that for an arbitrary value of β, the double integration of C results in a total area other than zero due to the term A'. However, for $\beta = \alpha^{-1}$ the term A' disappears and the double integration results in zero total area because D' has an equal zero area. The double integration of the linear combination of C is present in Figure SI-3. As can be seen, only $\beta = 2$ results in a flat and zero baseline, as expected by $\alpha = 0.5$.

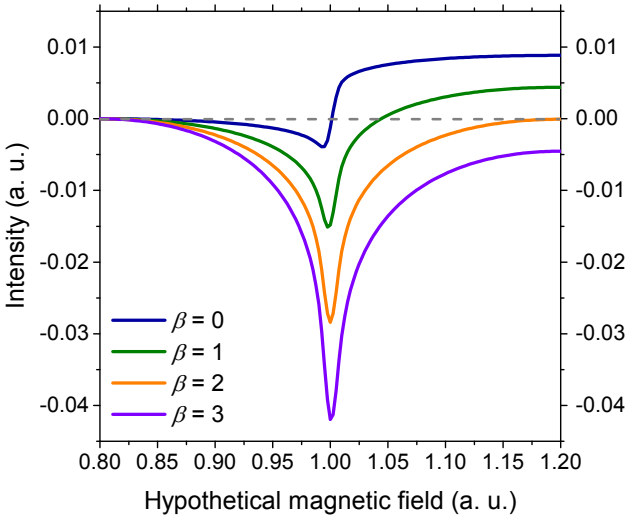

Figure SI-3. Double integration of C for different values of β.

As a real example, we applied the above procedure in an experimental NFMel HFEPR dispersion spectrum (S_{NFMel}) and its calculated Hilbert transform (H_{NFMel}), see Figure SI-4(a). We than take a linear combination of S_{NFMel} and H_{NFMel} following Eq. III. The double integration of the linear combination of C_{NFMel} with different values of β is shown in Figure SI-4(b).

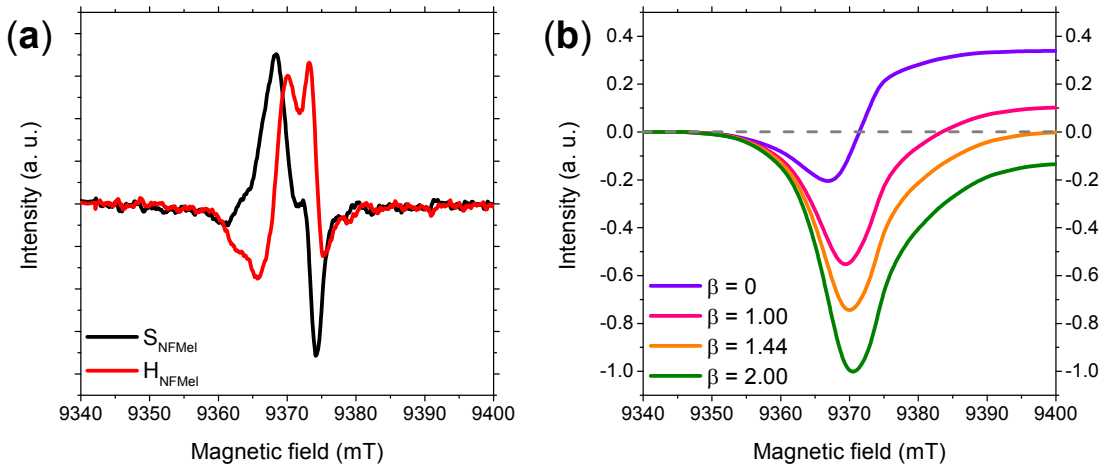

Figure SI-4. (a) Dispersion HFEPR experimental spectrum (S_{NFMel}) and its Hilbert transform (H_{NFMel}). (b) Double integration of C for different values of β.

Based on Figure SI-4, it is possible to observe that a flat and zero baseline is obtained with β = 1.44. This implies that, considering relation from Eq. IV, α = 0.69. Thus, with relation in Eq I, we can get the phase-corrected HFEPR experimental spectrum.

REFERENCES

RS1 - Pasenkiewicz-Gierula, M.; Sealy, R. C. Analysis of the ESR Spectrum of Synthetic Dopa Melanin. *Biochim. Biophys. Acta* 1986, **884**, 510–516.

RS2 - Paulin, J. V.; Batagin-Neto, A.; Graeff, C. F. O. Identification of Common Resonant Lines in the EPR Spectra of Melanins. *J. Phys. Chem. B* 2019, **123**, 1248–1255.

RS3 - Paulin, J. V.; Batagin-Neto, A.; Meredith, P.; Graeff, C. F. O.; Mostert, A. B. Shedding Light on the Free Radical Nature of Sulfonated Melanins. *J. Phys. Chem. B* 2020, **124**, 10365–10373.

RS4 - Grady, F. J.; Borg, D. C. Electron Paramagnetic Resonance Studies on Melanins. I. The Effect of PH on Spectra at Q Band. J. Am. Chem. Soc. 1968, **90**, 2949–2952.

RS5 - Tipikin, D. S.; Swarts, S. G.; Sidabras, J. W.; Trompier, F.; Swartz, H. M. Possible Nature of the Radiation-Induced Signal in Nails: High-Field EPR, Confirming Chemical Synthesis, and Quantum Chemical Calculations. Radiat. Prot. Dosimetry 2016, **172**, 112–120.

RS6 - Zadlo, A.; Szewczyk, G.; Sarna, M.; Camenisch, T. G.; Sidabras, J. W.; Ito, S.; Wakamatsu, K.; Sagan, F.; Mitoraj, M.; Sarna, T. Photobleaching of Pheomelanin Increases Its Phototoxic Potential: Physicochemical Studies of Synthetic Pheomelanin Subjected to Aerobic Photolysis. Pigment Cell Melanoma Res. 2019, **32**, 359–372.

RS7 - Earle, K. A.; Budil, D. E.; Freed, J. H. 250-GHz EPR of Nitroxides in the Slow-Motional Regime: Models of Rotational Diffusion. *J. Phys. Chem.* 1993, **97**, 13289–13297.